

AN EXPERIMENTAL INVESTIGATION  
OF FLUID DYNAMIC INTERFERENCE FORCES,

BY

Carl J. Fahrner

Dissertation submitted to the Graduate Faculty of the  
Virginia Polytechnic Institute and State University  
in Partial Fulfillment of the Requirements for the Degree of

MASTER OF SCIENCE

in

Engineering Science and Mechanics

APPROVED:



Dr. D. P. Telionis, Chairman



Dr. W. W. Stinchcomb



Dr. J. E. Kaiser



Dr. D. Frederick, Dept. Head

February, 1977

Blacksburg, Virginia

LD

5655

V855

1977

F335

c. 2

## ACKNOWLEDGEMENTS

MS 4-7-77  
I wish to express my gratitude to Professor Telionis for his encouragement and help during the course of this research. Also many thanks are due to Mrs. Doris Jones for an excellent typing job.

This research was sponsored by the NASA-Langley Research Center under Grant NGR-47-004-090.

## TABLE OF CONTENTS

|  | PAGE |
|--|------|
| ACKNOWLEDGEMENTS.....  | ii   |
| TABLE OF CONTENTS.....   | iii  |
| LIST OF FIGURES.....   | iv   |
| INTRODUCTION.....  | 1    |
| CHAPTER I. INSTRUMENTATION AND CALIBRATION.....                                    | 7    |
| a. The Towing Tank.....  | 7    |
| b. Data Aquisition.....  | 11   |
| CHAPTER II. THE TOWING TANK AS A FACILITY FOR<br>MEASURING AERODYNAMIC FORCES..... | 18   |
| CHAPTER III. INTERFERENCE FORCES ON HIGHWAY<br>VEHICLES.....                       | 30   |
| a. Background Information.....   | 30   |
| b. Description of Experiment.....  | 37   |
| c. Results and Discussion.....   | 43   |
| CHAPTER IV. CONCLUSIONS.....   | 49   |
| REFERENCES.....  | 50   |
| VITA.....  | 52   |

## LIST OF FIGURES

| FIGURE |  | PAGE |
|--------|--|------|
| 1      | Carriage speed calibration curve.....  | 10   |
| 2      | Detail of instrumented light strut.....  | 12   |
| 3      | Detail of instrumented heavy strut.....  | 13   |
| 4      | Typical recorder output.....   | 15   |
| 5      | Comparison of light and heavy strut data.....  | 16   |
| 6      | The effect of the wall on drag.....  | 21   |
| 7      | The effect of the free surface on drag.....  | 23   |
| 8      | Schematic sketch of a barge.....   | 24   |
| 9      | Wave drag reduction attempted with large<br>barge.....   | 26   |
| 10     | Wave drag reduction attempted with small<br>barge.....   | 27   |
| 11     | Artificial roughness tests using sand.....   | 29   |
| 12     | Schematic sketch of carriage and model.....  | 33   |
| 13     | The model car.....   | 34   |
| 14     | The model truck.....   | 35   |
| 15     | Isometric of the car and truck arrangement....   | 41   |
| 16     | Car and truck spacings.....  | 44   |
| 17     | Interference side force coefficients simu-<br>lating a passing process for three different<br>spacings, Y, under the influence of a<br>cross wind, with car, truck, and cross-wind<br>speeds of 70, 50, and 20 MPH respectively..... | 45   |

| FIGURE | PAGE   |
|--------|--|
| 18     | Interference drag coefficients for condi<br>tions of Figure 17..... 48 |

## INTRODUCTION

The aerodynamic property of drag, that is the force exerted on an object placed against a stream of water or air, was probably the first fluid dynamic force to become obvious to man. A late reference to this, in the middle of the nineteenth century, was made by Lilienthal [1] when he called every force caused by flow "widerstand." Drag is defined as the force component, parallel to the relative approach velocity, exerted on the body by a moving fluid. Lift and side force are fluid force components on a body in the vertical and horizontal planes, respectively, at right angles to the relative approach velocity. In this investigation we will be interested primarily in drag and side forces.

These forces can be measured on models in wind tunnels or water towing tanks. There are advantages and disadvantages when using water or air as a testing medium. One of the basic questions we pose is: can the towing tank be used to perform aerodynamic tests? In particular: is it possible to model properly interference forces between bluff bodies? The main objective of this investigation was to experimentally determine whether a towing tank can be used for aerodynamic tests. To address this question an investigation was carried out using tests run in the Virginia Polytechnic Institute and State University (VPI & SU) towing tank. The body shapes chosen

were those for which independent results from tests in air were available.

Tests in air are relatively simple. Prototypes can be tested in full scale using "coast down techniques," [2] or models can be scaled down and tested in wind tunnels. For incompressible viscous flows, Reynolds number scaling is the most important scaling factor. This number is the ratio of the inertial forces to the friction forces. Aerodynamic similitude requires that the model and prototype Reynolds numbers be the same

$$R_p = \frac{U_p L_p}{\nu_p} = R_m = \frac{U_m L_m}{\nu_p}$$

where  $U$ ,  $L$ , and  $\nu$  are the velocity, characteristic length, and kinematic viscosity respectively. If the same medium is used in the prototype and model flows, then with the characteristic length reduced to one tenth of the prototype value, the velocity must be increased by a factor of 10. For example, if a prototype is traveling with a full-scale speed of 60 miles per hour, the model must travel at 600 miles per hour to satisfy the Reynolds number criterion of similarity. This is strictly out of the question in air. At a speed of 600 miles per hour, compressibility effects, totally absent from the prototype situation, interfere with the modeling of the phenomena involved. However, it is known that dynamic similarity is still conserved, even when the two Reynolds numbers are



not equal, if they are both larger than the critical Reynolds number. In plotting the drag coefficient versus the Reynolds number, this property appears in the form of an asymptotic tendency to reach a constant value, as we will describe later.

Sometimes using a different medium than the prototype medium will aid in Reynolds scaling. For instance, if water is used to model airflow, the kinematic viscosity is decreased by a factor of 15, so that a one-tenth scale model traveling 60 miles per hour in air would only have to travel 33 miles per hour in water. Traveling at this or higher speeds in water quickly generates another difficulty: cavitation. Cavitation occurs when the pressure on a submerged vehicle drops below the vapor pressure of the water and a vapor cavity appears. The cavity shields a certain area from viscous forces and dynamic similarity is destroyed. The assumption that the drag coefficient is independent of the speed for larger Reynolds numbers has to be made again so that testing in water can be conducted at reasonable speeds. In the present experiments special care was taken to stay away from parameter values that overlap with the problem areas described.

Testing in water also lends itself well to some types of flow visualization techniques. Dyes [3], hydrogen bubbles [4], and solid particles [5] have been

successfully injected into flows to show patterns, wake boundaries, etc.. We have attempted some visualization experiments using dyes. In most of our efforts though, the dye jets were very unstable and the streamline patterns were not clearly exposed.

In addition to the flow pattern, the forces must be measured accurately. Standard methods for measuring aerodynamic forces are the use of pressure transducers, mechanical balances, and electronic balance systems employing strain gauges. Pressure transducers are placed on the model to be tested with their pressure sensing head flush to the surface. These devices then measure pressure at discrete points. Pressure can then be integrated over the area of the body to give the force acting on the body. This is a good method because it gives discrete pressures at individual points, which are necessary for some types of applications. Pressure transducers pick up small pressure differences and their signals are usually heavily laden with noise so that filtering is usually required. Moreover, they are very expensive and require a large amount of electronic support equipment. Our tests did not require discrete pressure point information, and this method was not considered.

Another method of measuring forces is the use of mechanical balances. The model is mechanically coupled to a weight balance which is hand balanced during the

test. This type of testing is simple and easy but only practical for steady flows and static experiments.

A third method of testing is accomplished with balance systems employing strain gauges that are calibrated to measure forces directly. The strain gauges are usually attached to a strut which in turn holds the model in place. This system allows for continuous data retrieval and on-the-spot monitoring. A problem sometimes encountered with this type of system is vibration (noise). It was found that a stiff strut could be used to eliminate much of this vibration.

Aerodynamic forces on surface vehicles have played a minor role in the development of the modern automobile. This is due to the fact that drag reduction affects only mildly the fuel economy and only at faster highway speeds. In the mid-sixties the automobile market was primarily interested in performance and comfort. Fuel was relatively inexpensive and energy consumption was of little concern. However, recently the automobile industry has started to emphasize economy. This trend can be expected to continue. The need for more economical vehicles as well as the concern over vehicle stability and safety necessitated the study of aerodynamic effects in recent years. Such studies have been mostly directed toward the reduction of drag on commercial vehicles [6-8], or the stability characteristics of isolated vehicles [9-11] or articulated trucks [12].

More recently a study was undertaken to assess the significance of aerodynamic interferences between two vehicles [13].

In response to the drive for automobile economy, aerodynamics should have become the focus of research; yet much of this field still remains unexplored. More attention is justified since lighter vehicles will reduce friction and tire losses significantly, and leave the aerodynamic forces the most dominant resistant forces, at least at high speeds. An area that is being investigated with new intensity is automobile aerodynamic stability [14]. With the introduction of light-weight cars, cross winds and aerodynamic effects from passing vehicles will become a real threat to passenger safety. For example, if a typical automobile's weight is reduced by one half and it encounters a strong cross wind, its side-slip velocity will be approximately four times as big as that of a normal-weight car. This will be extremely hazardous to small cars since they already experience much erratic lateral movement from winds and passing trucks. As a practical application of the experimental methods developed, we will be concerned with automobile safety, the study of aerodynamic disturbances, and in particular, the way in which cross winds affect automobile handling.

## CHAPTER I

### INSTRUMENTATION AND CALIBRATION

#### a. The Towing Tank

The major testing device in this set of experiments was the Virginia Tech towing basin [15]. This basin is made of reinforced concrete painted with a chemical and moisture resistant enamel. The width of the basin is 6 feet and the maximum water depth is 4 feet. The overall length of the basin is 98 feet but the first four feet and the last 24 feet are used for braking the carriage. The usable test length is then approximately 70 feet. There are two glass-walled observation pits along the side of the tank, one located approximately in the middle of the test region and the other located at the starting end. The observation pits will be used later in our present project with the Department of Transportation for flow visualization experiments.

The carriage rails were designed and constructed by Kemp and Remes of Hamburg, Germany and shipped in subassemblies to VPI. Each rail was leveled to a water surface, set on 52 supports, and because of the short length of the tank, no correction in rail height for earth curvature was needed. A 400 Volt DC motor drives the carriage through a two-gear reduction box. The DC power is supplied from a 220 Volt AC motor-generator set.

With the gear-box in position I, a maximum speed of the carriage of 0.22 meters per second at 3000 RPM can be obtained. With the lever set in position II, a maximum speed of 3.0 meters per second at 3000 RPM can be obtained. For more precise speed control in the low speed range, the DC motor can be switched to a maximum of 1500 RPM at full voltage. The speed of the carriage can be controlled to within fine units with the carriage operating in "electronic control." This finer gauging of carriage speed is regulated by a tachometer-generator or by a feed back from the motor armature voltage. Using this device, a maximum acceleration of 0.7 meters per second per second can be obtained. The carriage can also be driven using the "hand control" rheostat, which gives less acceleration than the "electronic control," but has accurate speed settings. This method of speed control was extensively used in our experiments. A speedometer was also on the carriage but was observed to be inaccurate, and it was not used.

The speed and four other inputs can be recorded on a recording drum which uses writing magnets with ink pens for recording on graph paper. A wheel mounted on the rear of the carriage and rolling on the inside rail is made such that a current is sent to the writing magnets every 0.1, 0.5, or 1.5 meters travel of the carriage. A seconds-clock gives a current to the writing magnets every .2, 1.0, 3.0, or 6.0 seconds. Thus by recording travel of

the carriage and time simultaneously on the recording drum, a very precise measurement of speed can be obtained. In the present work, a high degree of accuracy in speed ( $\pm 0.01$  feet per second) was not necessary since we were looking for speeds above transition from laminar to turbulent flow. For this reason the "hand control" rheostat was calibrated periodically using the drum recording method described above. A calibration curve is shown in Figure 1. The periodic checks for drift of the speed settings have indicated an accuracy of  $\pm 0.1$  feet per second.

Braking occurs automatically at both ends of the tank, and the carriage can also be stopped by an emergency brake located on the console. The brake, which is also applied if power to the carriage is interrupted, is of the magnetic clutch type and brakes the DC motor directly with a deceleration of 0.7 meters per second per second.

All necessary voltages for operating the equipment are available on the carriage; this includes two 110 Volt AC outlets and two 12 Volt DC outlets.

A dynamometer, which is available to measure drag, can be used for measurement while the carriage drives at a constant speed, or it can be set to pull the model with a constant force while the carriage is adjusted so that the model maintains a constant position relative to the carriage. This facility though requires mechanical coupling between the model and dynamometer, and it was not

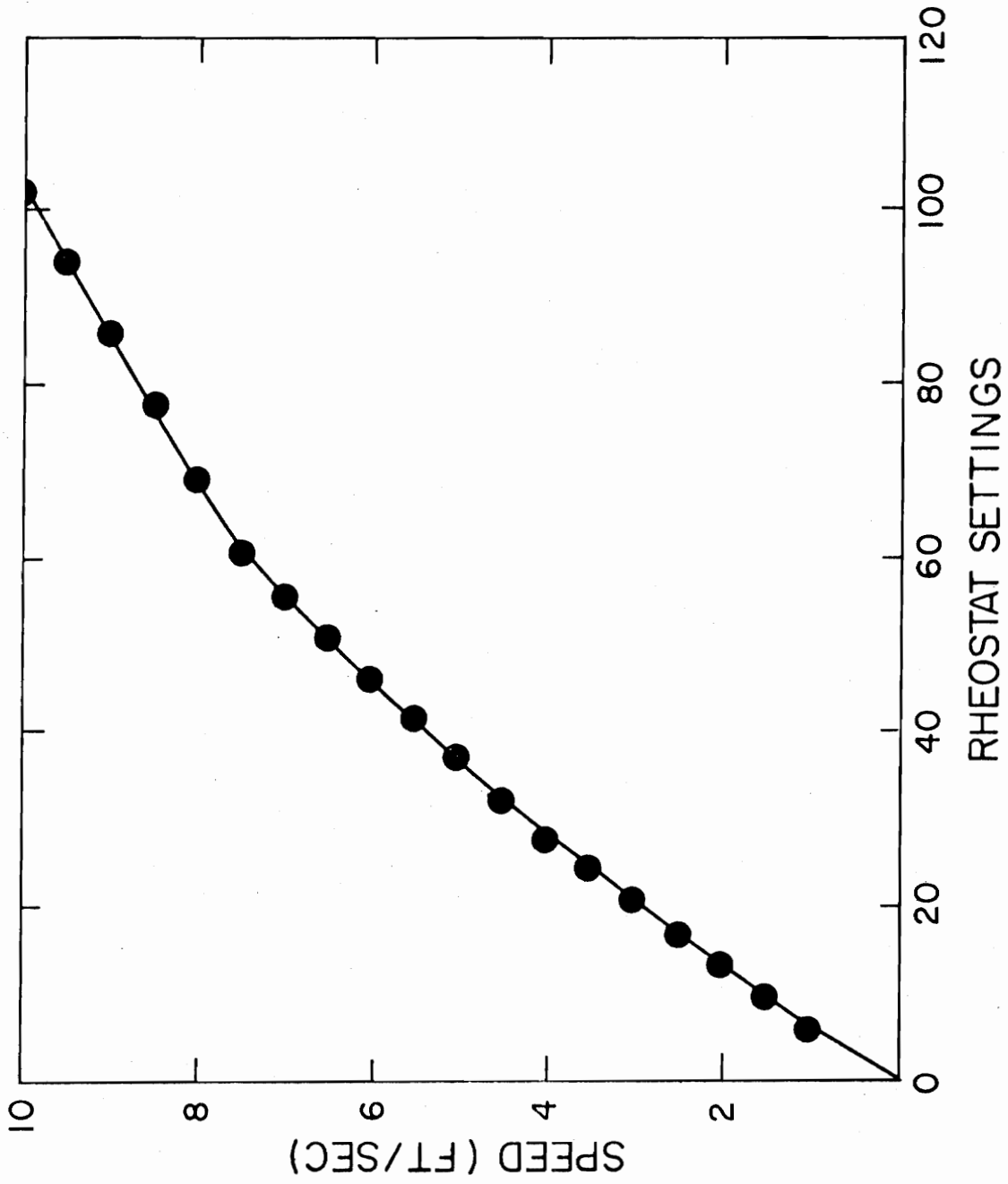


Figure 1. Carriage speed calibration curve



used in the present experiments.

#### b. Data Acquisition

Instead of using the carriage dynamometer which was not conducive for our tests, new balance systems were designed and constructed. They consisted of struts with a cross section of a symmetric airfoil. Strain gauges were attached and the system was calibrated to measure directly drag and side forces. Two different strut sizes were used with cross section chord lengths of 1 inch and 3 inches, and an aspect ratio of 12 and 4 respectively (see Figures 2 and 3).

MM strain gauges of EP-08-500 BH-120 gauge type were used, with a resistance of  $120.0 \pm .3\%$  OHMS, and a gauge factor of  $2.065 \pm .5\%$  at 75°F. Two gauges for each direction, mounted one on each side of the strut, were used to double the strain signal. The gauges were sealed in wax so that no moisture could affect their output. The gauge signals were amplified by a Vishay Instruments BAM-1 Bridge Amplifier and Recorder. The signal was recorded on a 2-Channel Hewlett-Packard 7100 B Strip Chart Recorder.

Strut calibration was repeated before every test. This was accomplished by clamping the strut down, hanging known weights at the appropriate location, and then adjusting the recorder output to read in pounds per inch

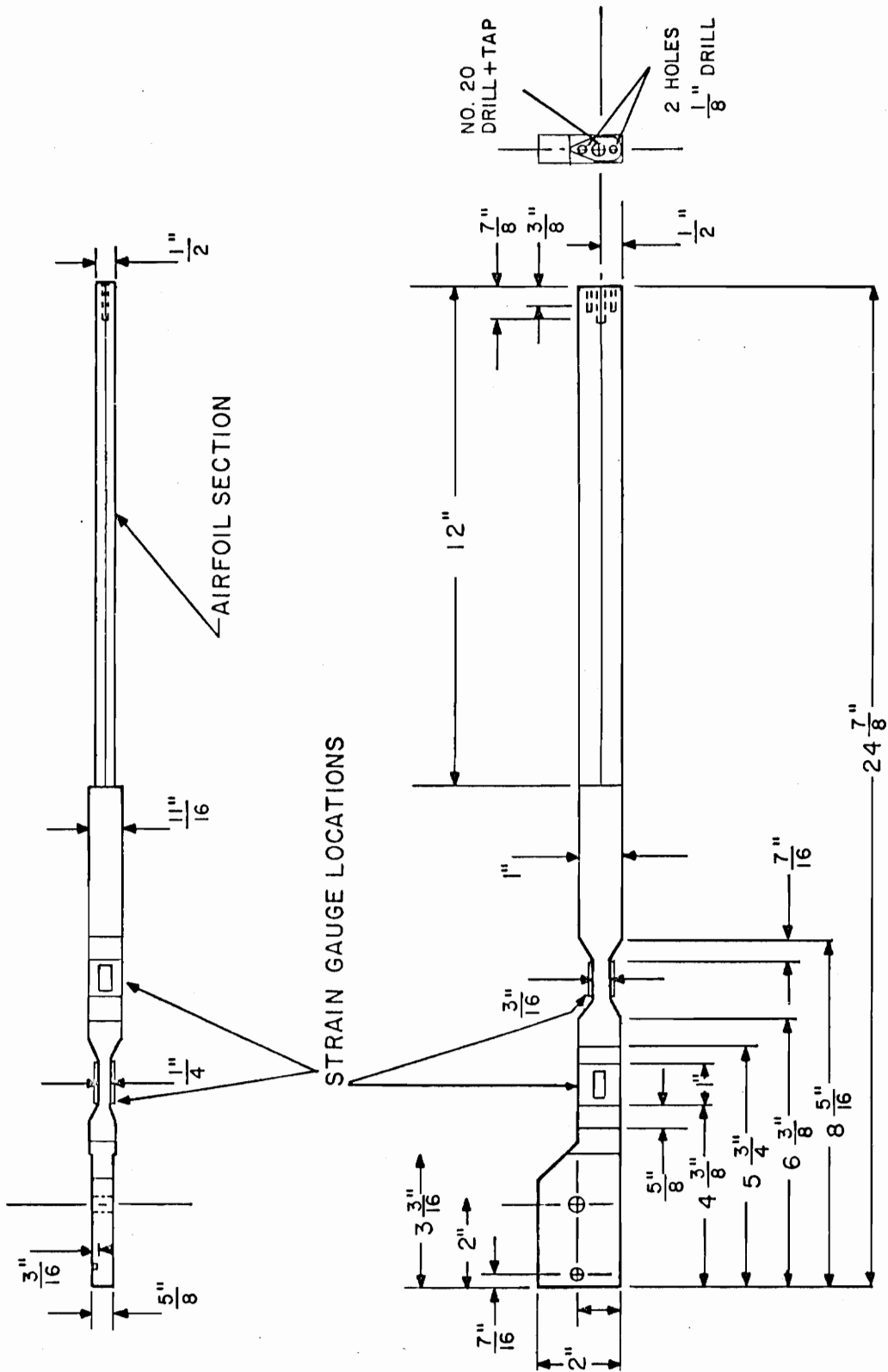


Figure 2. Detail of instrumented light strut

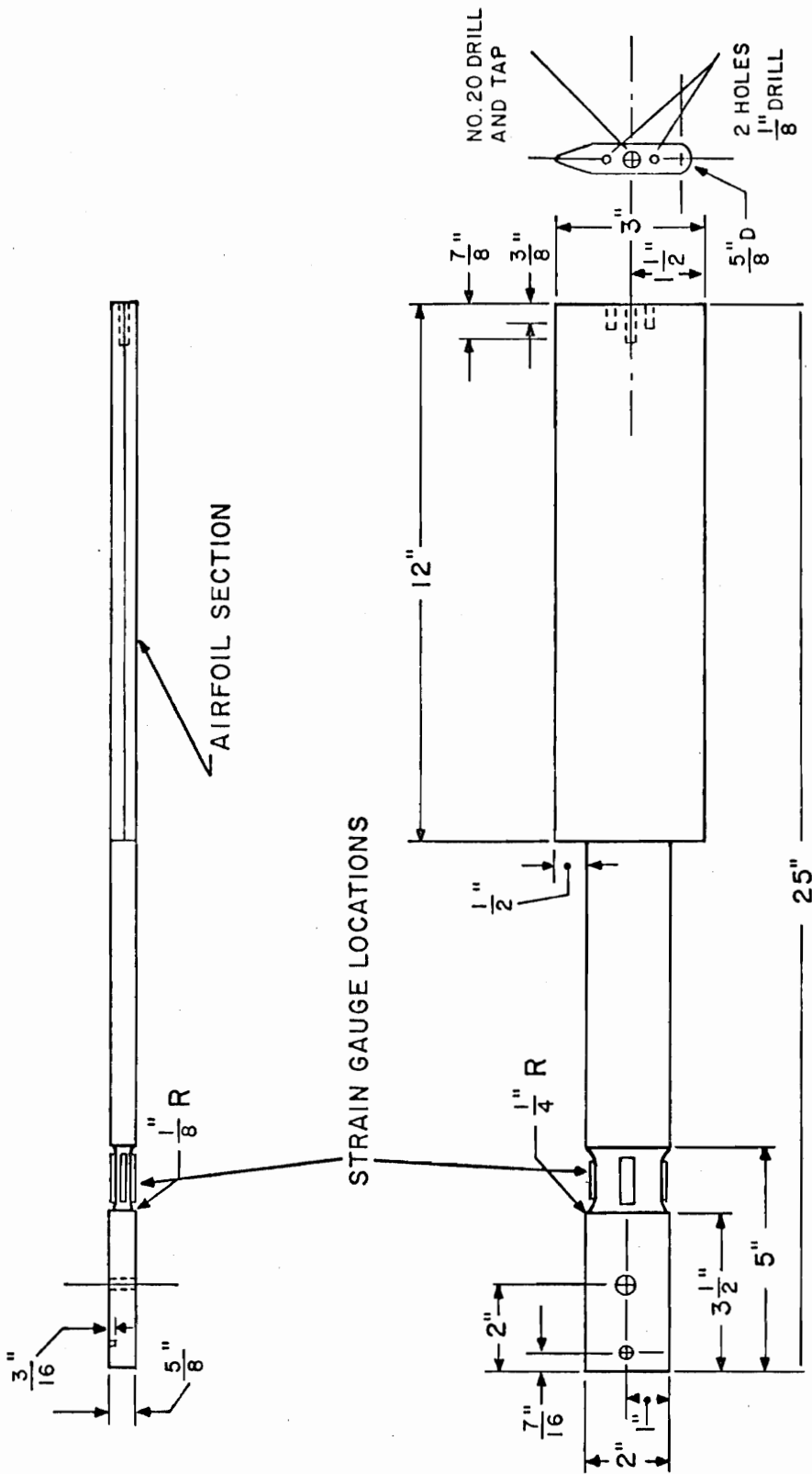


Figure 3. Detail of instrumented heavy strut

or other convenient units. The recorder pen was zeroed before each run and all recorder output was reduced manually. Three typical recorder outputs can be seen in Figure 4. The drag due to the strut alone was measured separately and then subtracted from the total drag of the strut and model.

In the first series of experiments the lighter strut was used, and it was observed that the hydrodynamic forces would induce vibrations of considerable amplitude. An average of the fluctuating drag measurements resulted in values substantially below the values reported in published experiments [7,16,17]. This is shown in Figure 5 where data received with the light and heavy strut are compared. More data than shown was gathered for drag reduction. Only one run, representative of the data, is shown for clarity. It appears that in the laminar region,  $Re < 3.0 \times 10^5$ , the reduction in the average drag is quite often on the order of one half its steady state (heavy strut) value. We attribute such a phenomenon to the nonlinearity of the boundary layer. It is well known that the location of separation is strongly affected by fluctuations of the mean flow [18]. It was conjectured that the forced fluctuations displaced the point of separation downstream, and thus reduced the size of the wake and the total value of the drag. This is a by-product of the present effort which may have significant

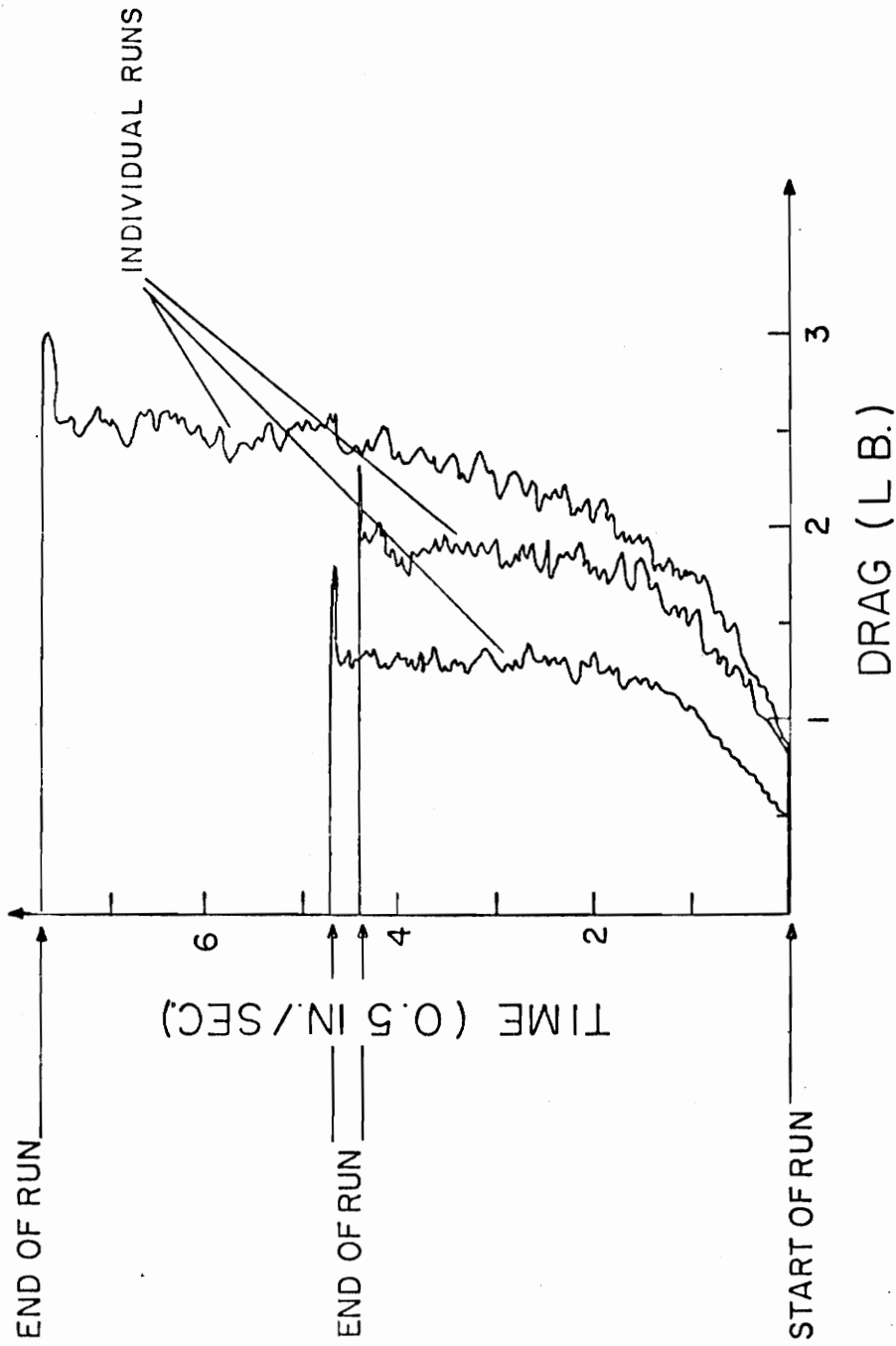


Figure 4. Typical recorder output

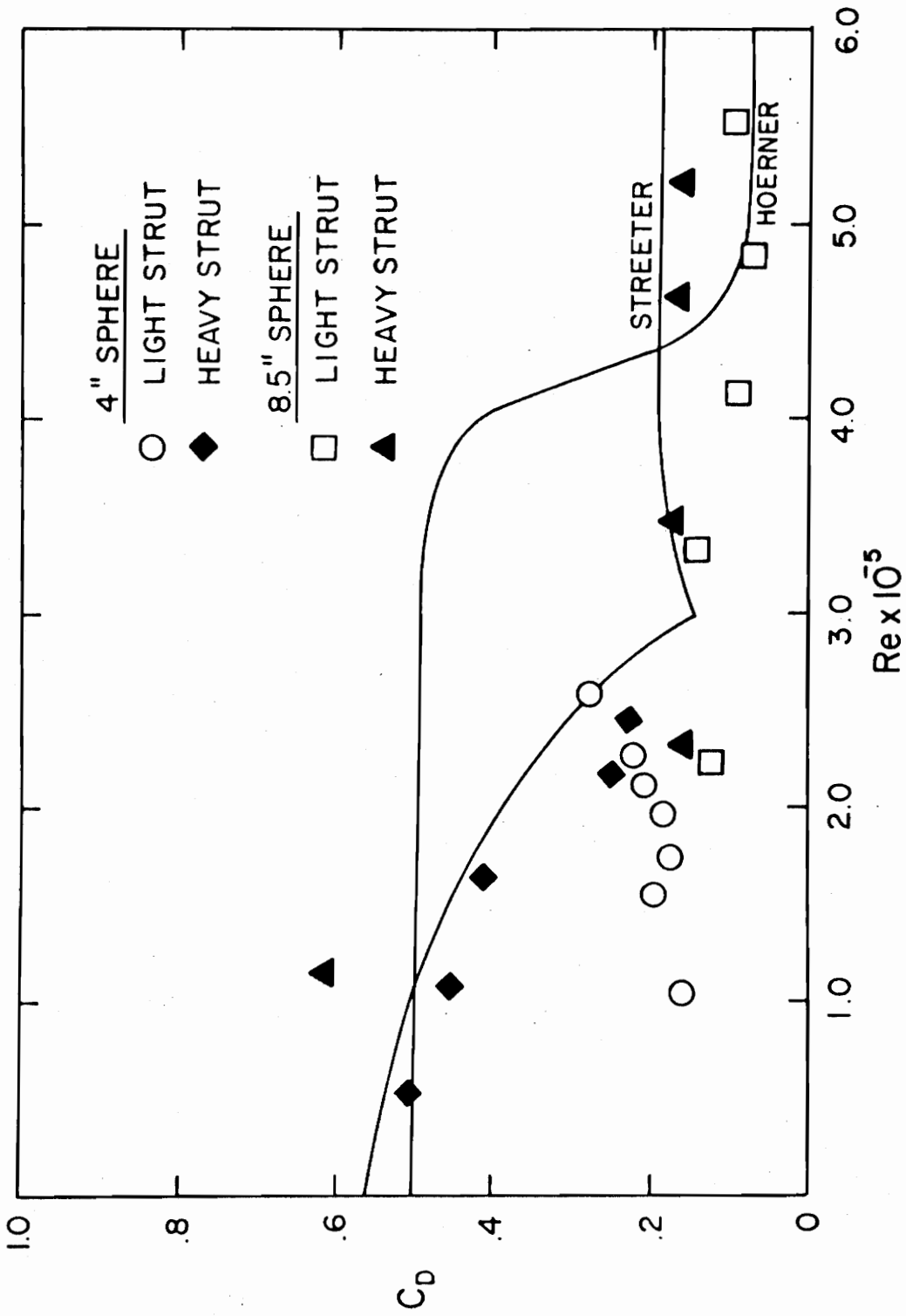


Figure 5. Comparison of light and heavy strut data

implications and therefore deserves further study.

Forced fluctuations offer a method for significantly reducing the drag on blunt bodies. It may not be a very appealing method for any type of transportation method, but it could find use in a variety of other applications.

## CHAPTER II

### THE TOWING TANK AS A FACILITY FOR MEASURING AERODYNAMIC FORCES

Towing tanks were designed originally for the testing of surface ships and were later used extensively for submarines as well. Very little use has been made of such facilities for aerodynamic tests of other types of vehicles. It appears that there are advantages and disadvantages in performing aerodynamic tests in water and in particular, towing tanks. The most critical feature of such tests is of course dynamic similitude. To model viscous effects properly, the Reynolds numbers of the model and prototype must be the same. With the kinematic viscosity of water 15 times smaller than that of air, we can afford to use water speeds 15 times smaller than would be necessary in air. However, real life speeds simulated in this way would still be rather low due to cavitation constraints. Speed is not a very stringent constraint though, because for Reynolds numbers above a critical value, that is for turbulent flow, the drag coefficient is usually assumed to be independent of the Reynolds number. On the other hand, proper model simulation in air requires speeds larger than the speeds of the prototypes and soon compressibility effects, that is Mach numbers above 0.6, become an influential factor to be taken into account. Such difficulties would not arise with water, except for



the phenomenon of cavitation which would appear at relatively higher speeds. Moreover, tests in a towing tank are absolutely free of problems inherent to air experiments such as free-stream turbulence, wall boundary layers, and secondary flow, since the fluid is actually at rest.

One of the main problems encountered when using the towing tank, is the blockage effect for relatively small facilities, that is, the interference of the rigid walls and of course the effect of the free surface. This chapter presents an experimental investigation of such effects; in other words, we seek to answer the question, "is it possible to use a towing tank for aerodynamic experiments?" To address the above question, tests have been conducted in the VPI & SU towing tank. In all these experiments spheres were used as models, in order to facilitate comparison with well-documented experimental results [7,16,17]. Two spheres 4.0 inches and 8.5 inches in diameter were used. The instrumented struts described in the previous chapter supported the spheres in place at depths of 2 to 10 inches below the surface.

In the first set of tests using the light strut, the sphere drag was approximately one half of what other experimental data indicate [7,16,17]. This was accounted for by induced fluctuations as mentioned in chapter one. A heavier strut was the answer to this problem, and data taken with that strut compared favorably to other

experimental data, as can be seen in Figure 5.

Next, the effect of the presence of a wall was considered. Such problems have been studied extensively [18-20] either for the most ideal cases of inviscid flows or for the most practical situations of ground effects on aircraft or automobiles. Our experiment consisted of towing a 4 inch sphere at various distances from one of the tank's vertical walls. The results in Figure 6 indicate that the drag decreases with distance from the wall. Most of the data points are clustered close together for distances greater than  $R/4$  from the wall, where  $R$  is the radius of the sphere. This is true for the smallest and largest Reynolds numbers tested, which correspond to laminar and turbulent boundary layers respectively. A larger spread appears in the middle region which corresponds to transition, a phenomenon that characterizes almost all of our experimental data. For a distance equal to  $R/4$  from the wall the increase of the drag is dramatic and is clearly indicated in Figure 6. The conclusion drawn from this experiment is that the effect of the wall in a towing tank is insignificant if the model is tested at a distance from the wall of at least one characteristic length.

In the next set of experiments, tests were conducted to measure the effect of the surface-wave formation on the wave drag. This clearly depends on the

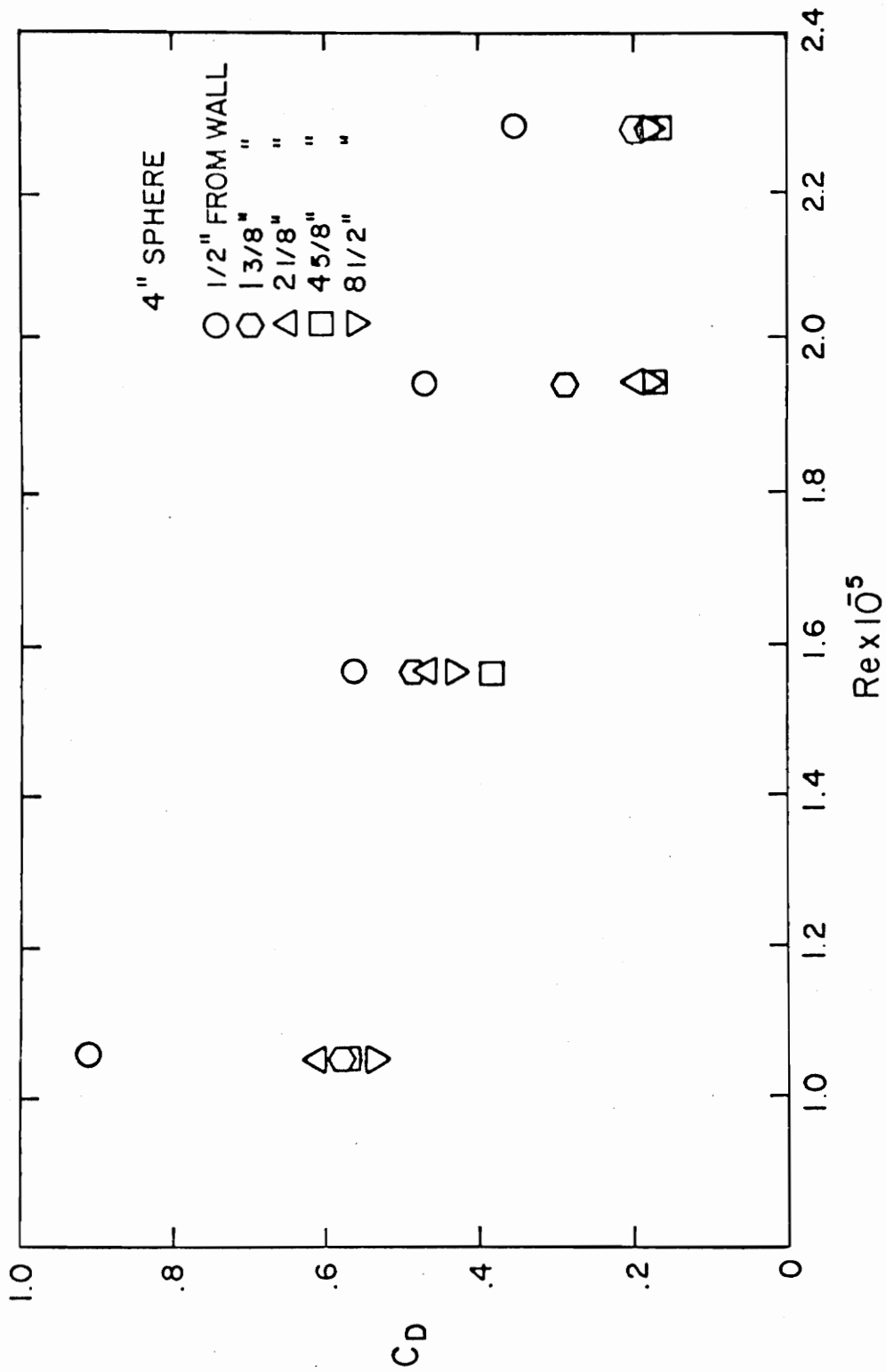


Figure 6. The effect of the wall on drag

configuration of the body and our results hold exclusively for spheres. To determine the surface effect on the drag, the two spheres were run at depths of 2, 4, 6, and 8 inches from the surface, at speeds of 2, 4, 6, 8, and 9 feet per second. For the most part, Figure 7 shows that a sphere with artificial roughness has almost constant drag for depths of 4, 6, and 8 inches, but increases slightly at a depth of 2 inches. Both smooth and roughened spheres were examined. However, roughened spheres were used to mask the transition effects. For depths less than 2 inches and of course for partial submergences of the body, the drag due to wave formation increases substantially, but this is beyond our interests here. In conclusion, a depth of  $D/2$  seems to be a safe distance for tests free of surface effects, where  $D$  is the diameter of the sphere or characteristic length of any similar size blunt object.

In an attempt to suppress completely the formation of surface waves, two barges were designed of sizes 24 X 42 inches and 64 X 84 inches respectively. These were constructed of plexiglass and allowed to float over the model as shown schematically in Figure 8. For slow speeds, the barges were simply towed over the model. For higher speeds though, that is in the range of speeds which cause considerable wave action, dynamic pressures developed that gave the barges a considerable angle of attack. As a result, the flow field was distorted. This was avoided

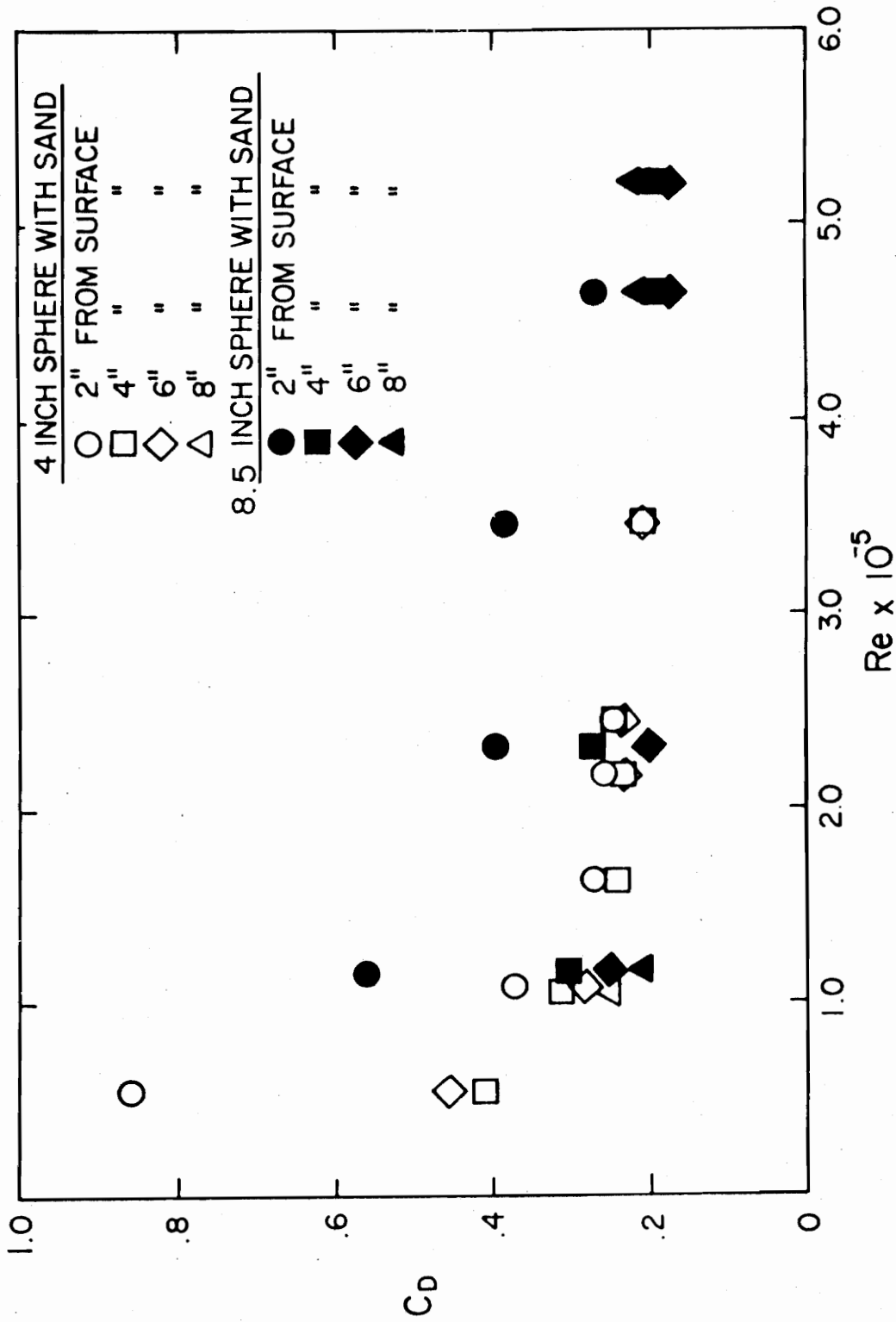


Figure 7. The effect of the free surface on drag

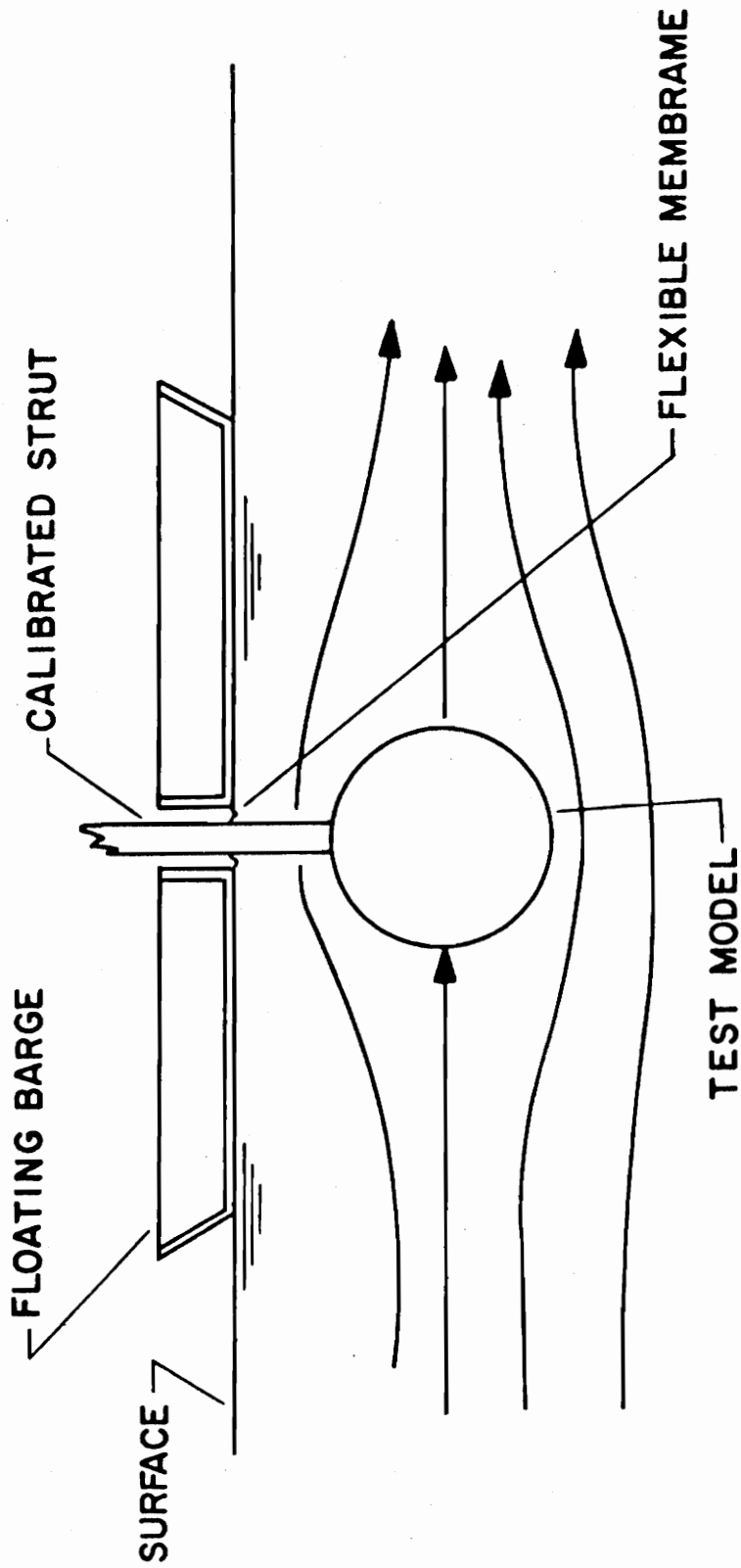


Figure 8. Schematic sketch of a barge

for the most part, by securely connecting the barges to the carriage, although the barges still tended to "bow" slightly at high speeds. Figures 9 and 10 show the results of tests performed with the large and small barge respectively, as well as the no barge data for comparison. Tests with the large barge yielded no obvious decrease in drag as suspected, probably because the large barge itself generated a lot of waves. The small barge did for the most part suppress the drag slightly but not enough to warrant further attention.

In addition to the strut fluctuations, wall effects, and surface effects, we also had to resolve the fact that almost all real life situations that we would like to simulate in our laboratory, correspond to Reynolds numbers of the order of  $10^6$ - $10^8$ , which we cannot duplicate. We emphasized before that if the flow is turbulent, the aerodynamic forces are independent of the Reynolds number. Therefore, to simulate correctly a high Reynolds number situation, it suffices to force the boundary layer over the model to become turbulent. We have accomplished this in our experiments by using artificial roughness. It was found that if extensive areas of the front of the spheres were covered with sand, the drag increases instead of decreasing, most probably due to the expected increase of shear stress due to roughness. If only a small area, approximately 1 square inch on the small sphere or 2 square

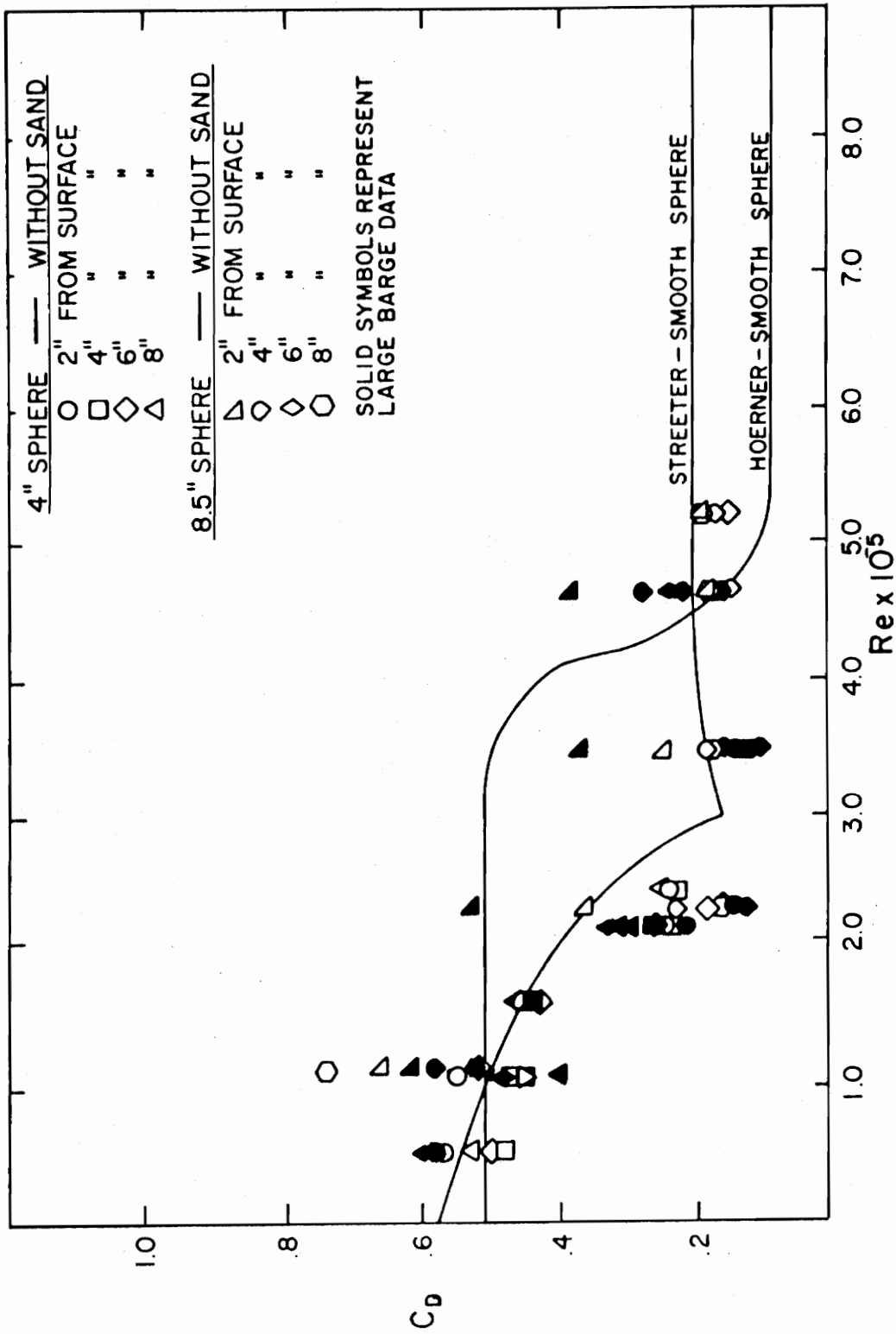


Figure 9. Wave drag reduction attempted with large barge



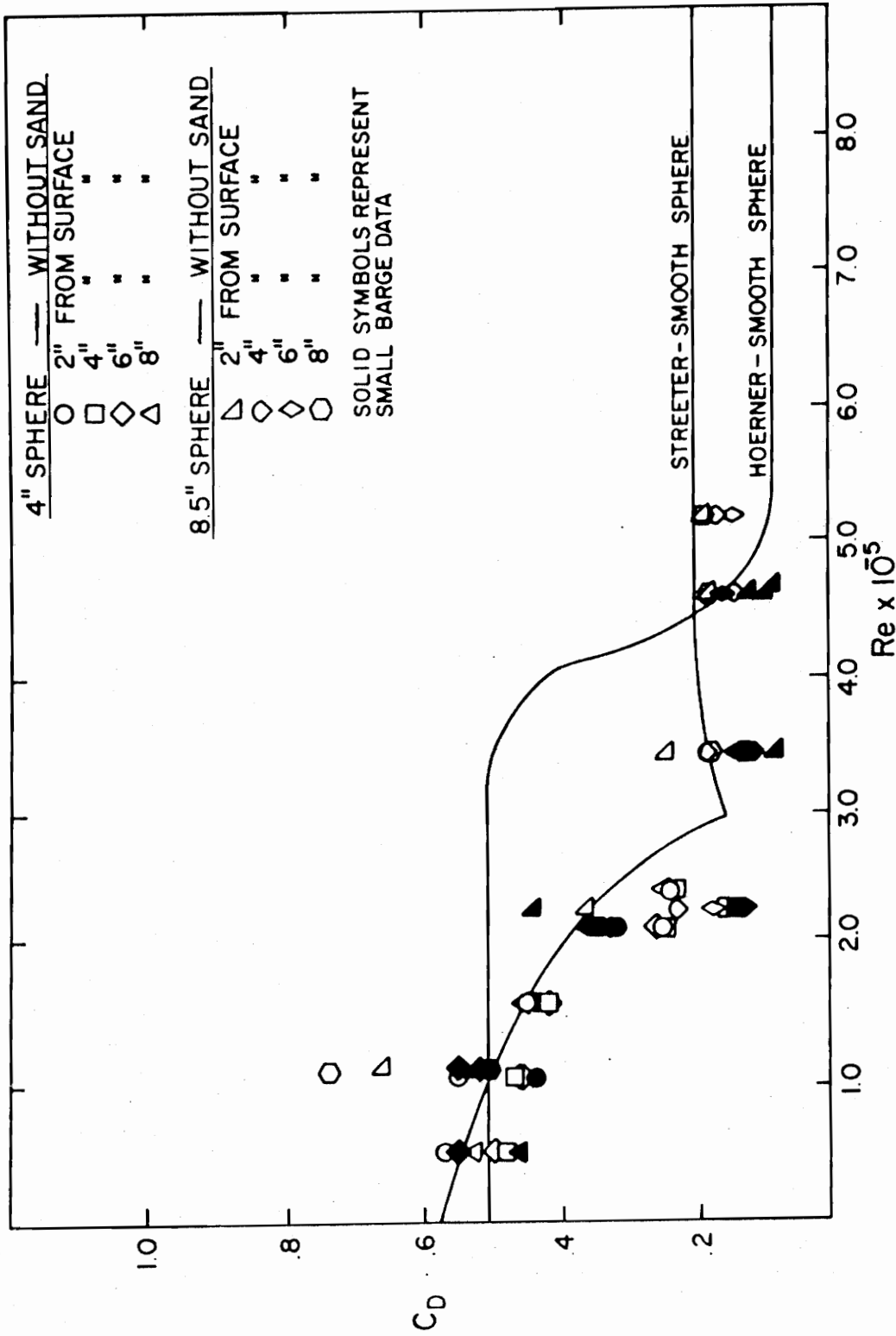


Figure 10. Wave drag reduction attempted with small barge

inches on the large sphere, is given artificial roughness, then the drag is reduced to the turbulent flow level for Reynolds numbers as small as  $Re=10^5$ . This is clearly seen in Figure 11 where we show data with and without artificial roughness. The neighborhood of transition is clearly shifted to lower Reynolds numbers, and in fact it appears more clearly defined. In all the measurements that follow, special care was taken to make sure that the boundary layers were properly tripped, and that the flow was turbulent.

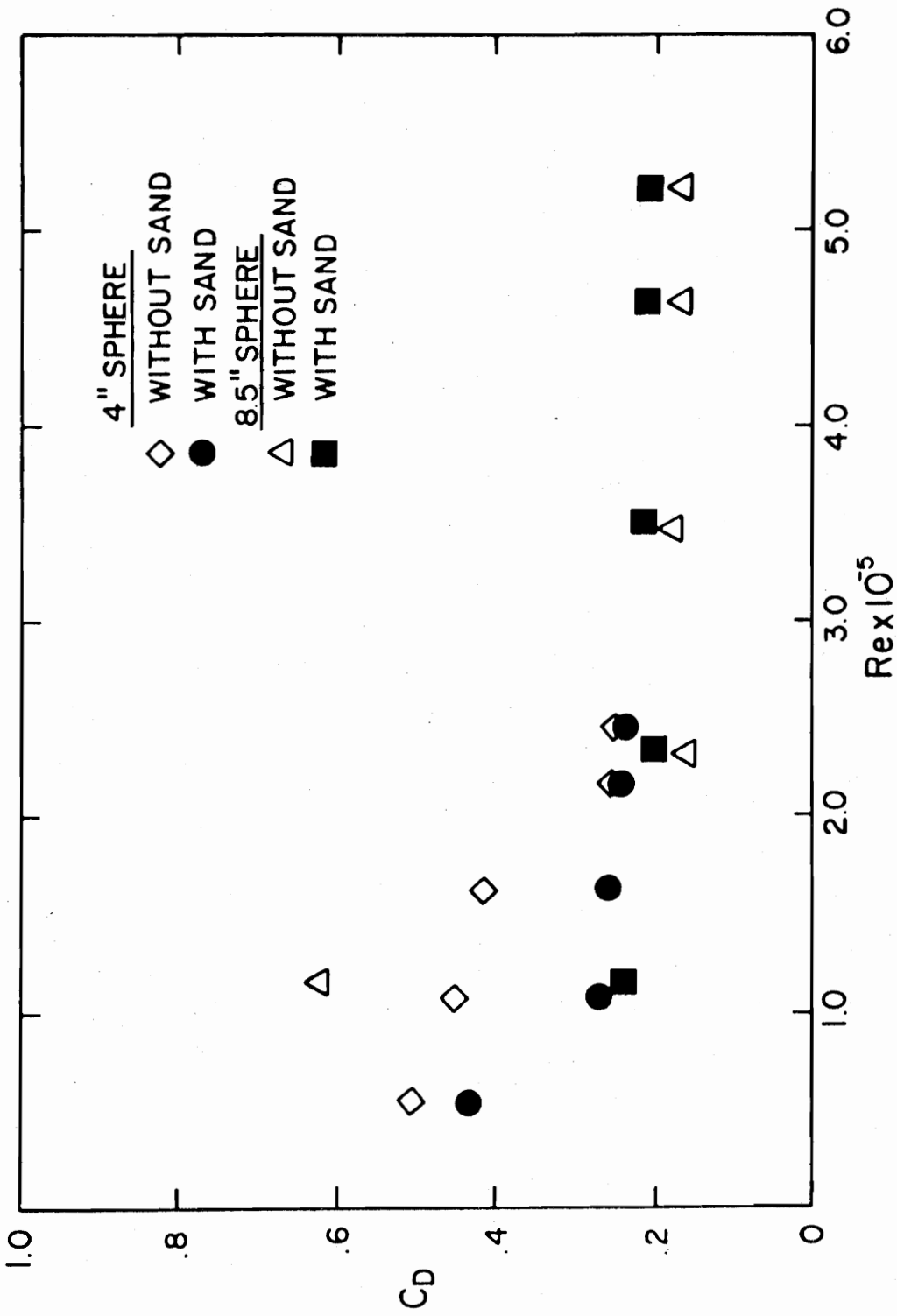


Figure 11. Artificial roughness tests using sand

### CHAPTER III

#### INTERFERENCE FORCES ON HIGHWAY VEHICLES

##### a. Background Information

The importance of aerodynamic forces and in particular the need for reduction of drag, first came to the attention of automobile manufacturers in the 1930's. Oldsmobile came out with their Airflow Series [22] in 1934. This car had a wind-tunnel-tested body and was the first car ever produced that had less drag traveling forward than backwards, by design. The Airflow Series did not sell very well because of their unusual shape for that day. However, it did cause manufacturers to realize the importance of aerodynamic drag.

Many road tests have been conducted to measure the drag of an automobile or truck according to the principle of "drag equals mass times deceleration" [8]. Of course this type of test includes the drag due to the tires and mechanical system. Additional tests performed on special stands are required to determine the drag due to mechanical friction which is then subtracted from the total drag to give the net aerodynamic drag.

Wind tunnels can be used to measure the drag of automobiles either by testing models or by placing the vehicles themselves into large wind tunnels. In these tests and contrary to normal operation, wind is blown

against the automobile. Perfect geometrical model configurations and proper representation of the road surface, which in reality is not fixed in relation to the vehicle, are the primary concerns in wind tunnel tests.

Representation of the ground has always been a problem when testing scale models. There are different methods for modeling this effect [7], as for example the use of a flat plate, the method of two mirror images, or a belt moving at the speed of the medium. The simplest reproduction of the ground effect is the use of a flat plate placed under the testing vehicle. However, even the plate produces a boundary layer, which can considerably alter the flow pattern around the model. A fixed ground plate usually leads to drag coefficients slightly higher than proper simulation of the road surface. To avoid the ground-plate interference, attempts have been made to remove the boundary layer by sucking it away through a porous plate. Even so, the drag coefficient remains too high. With the image method, the ground plate is omitted entirely. A second identical model is placed upside down with its wheels against those of the first model. Theoretically, because of symmetry, no particles will pass through the imaginary road surface between the models. Actually, since the flow between the models may be turbulent and separated, asymmetric growth of vortices may violate the symmetry of the system. Also the vortex

system behind the models will be affected since there is no real surface to offset vortex formation. A flat plate placed behind the vehicles in the plane of symmetry will alleviate some of the erroneous vortex formation. The best but most difficult way to reproduce the effect of the road in a wind tunnel or towing tank is by the use of a belt, moving at the same speed as the test medium, placed close to the wheels. Drag coefficients obtained in this manner are most representative of full-scale results.

In the present tests we used the image method with no vortex plates. This method seems to be most practical if crosswinds are to be simulated by setting the models at an angle  $\alpha$  to the carriage direction. The models were then towed at this angle and dynamically passed by one another as shown in Figure 12. This was accomplished by constructing a second smaller carriage built to fit on the larger towing carriage. Vortex plates were not used because the angle at which the vehicles were set would not permit the plates from eliminating downstream vortex crossover. All vehicle models were made out of wood and simulation of fine detail was not attempted (see Figures 13 and 14). The vehicles, approximately 1/21 scale, were designed to simulate the geometrical configurations of a car and truck so that general aerodynamic trends could be investigated.

In the present work we have tried to estimate the

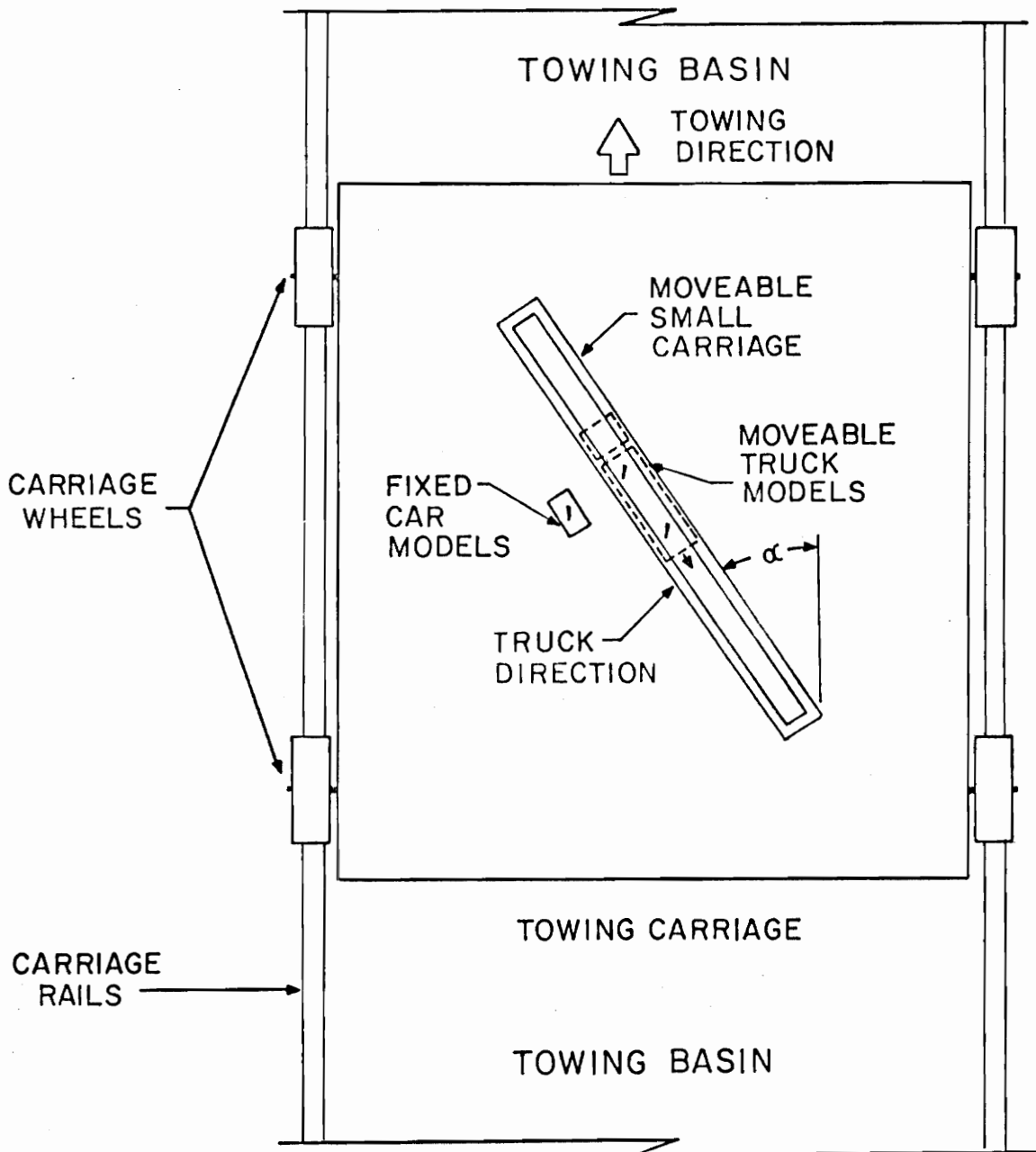


Figure 12. Schematic sketch of carriage and model

$\frac{1}{4}$ " RADIUS ON ALL EDGES

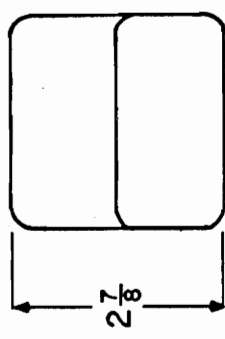
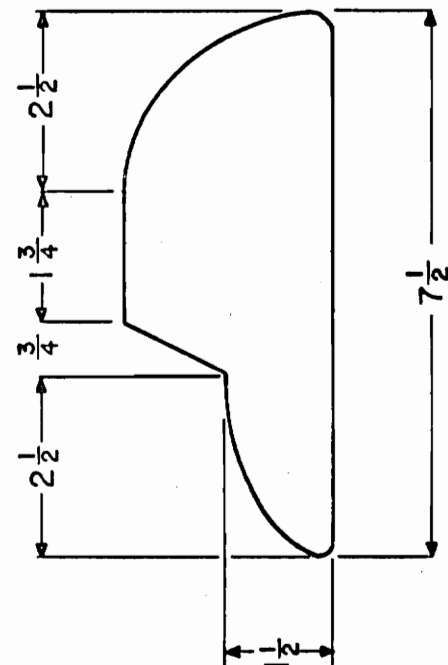
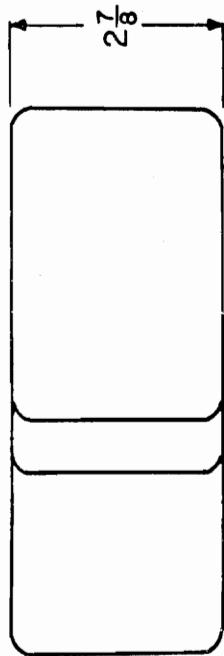


Figure 13. The model car



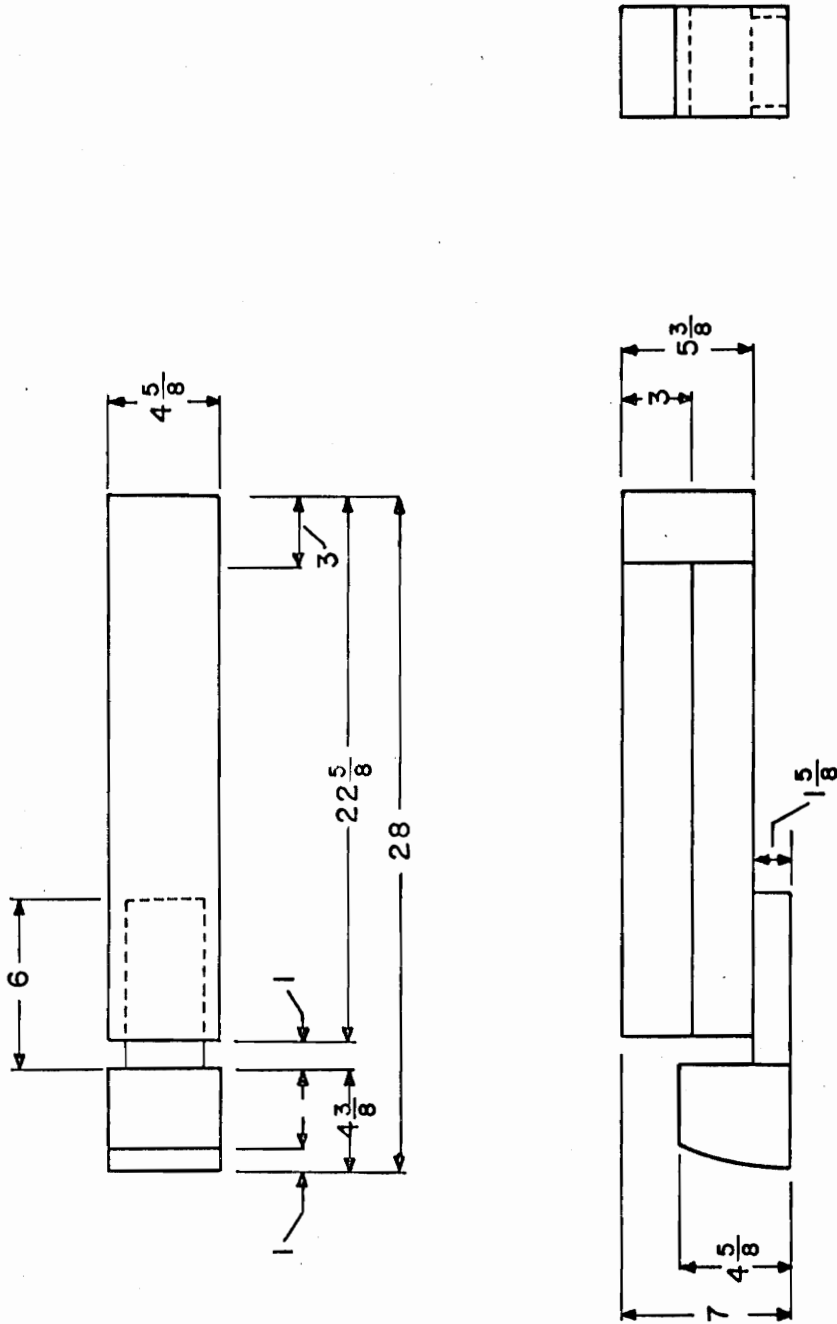


Figure 14. The model truck

reliability of our data, by comparing the present results to earlier experimental information. In the first two chapters we compared our results to data reported by Hoerner [7] and Streeter [16]. In this chapter we will compare our results to Brown and Seemann's [13] highway interference data. Brown and Seemann modeled a number of typical highway situations, some of which are of interest to us. Their objective was to measure the aerodynamic disturbance effects on a range of typical passenger vehicles caused by buses and trucks operating in close proximity to the passenger vehicles over a range of ambient wind conditions. Each test situation involved two vehicles in one of three modes; passing, being passed, and passing in opposite directions. The disturbed vehicle containing a wind-tunnel balance, associated signal amplifiers, and telemetry system, was referred to as the metric model. The disturbing vehicle model was not instrumented and served only to create the aerodynamic disturbance. The metric models included a 1970 Ford Torino, a 1967 Volkswagon Sedan, and a 20 foot Kenskill travel trailer in towing position behind the Ford Torino. The disturbing models were MC7 and MC6 buses manufactured by Motor Coach Industries and a Ford COE tractor with a 40 foot long, 96 inch and 102 inch wide semi-trailor. The total length of the tractor trailer was 51 feet. All models were one tenth scale and traveled at full scale

speeds. Ambient wind levels of 0, 20, and 40 MPH were created for each vehicle combination and passing mode. The equivalent full-scale lateral spacings between the centerlines of the two vehicles were 8, 10, and 12 feet respectively. The dimensionless parameter used to measure relative lateral spacing between the models was  $Y$ , where  $Y$  was "car widths" of the metric model. The relative longitudinal position of zero was taken as that position where the vehicles first intersect each other as viewed from the side. The dimensionless parameter used to measure the relative position of the models was  $X$  or simply "car lengths" of the metric model. We have attempted to duplicate their Reynolds numbers, cross winds, spacings, and dimensionless parameters wherever possible. We will be mostly interested in Brown and Seemann's tests of a Volkswagon model traveling at 70 MPH and passing a truck traveling at 50 MPH with an ambient cross wind of 20 MPH.

#### b. Description of Experiment

To reproduce Brown and Seemann's results [13] we fabricated two sets of models: a Volkswagon and a 98 inch wide, 49 foot tractor trailer as seen in Figures 13 and 14.

At first it was attempted to test the drag coefficient for a single model, roughly simulating a Volkswagon. The first test was conducted by fastening the

top of the model to the end of the strut, and then running the car in the tank with no ground simulation. The drag coefficient obtained in this manner appeared to be almost twice as high (.77) as compared to Brown and Seemann's prediction (.45). To investigate whether turbulence effects were accurately simulated, artificial roughness (sand) was applied to the nose of the model. The second test did not produce the expected drop in drag, instead the drag coefficient remained approximately the same (.76). It is believed that at or below the critical Reynolds number and for small models, the tripped boundary layer relaminarizes and the effect of roughness is almost eliminated. Alternatively, coarse artificial roughness (1/4 inch screen) was applied to the nose of the model to generate turbulence that would pertain over the entire model. This method resulted again in a slight decrease of the drag (.73) as compared to the drag measured in the first experiment without a screen, but not as much as expected. At this point it was realized that we did not need the screen on the nose of the car as much as we needed it on the rear window area to generate turbulence right at the point of separation. Again, as before, this did not prove to be very effective, and a drag coefficient of .71 was measured. Next we mirrored the models by holding them apart with two 0.25 inch steel rods in order to simulate the correct position above the plane of

symmetry. The drag measured in this way was found to be unacceptably high (.65).

It was then conjectured that the heavy strut connected to the top of the model was interfering with the wake formation, thus generating larger drag coefficients. To correct this we positioned a  $3/8$  inch diameter sting into the rear of the car. This sting extended  $2\frac{1}{2}$  inches from the rear of the model and then made a  $90^\circ$  bend to come up 6 inches and fasten to the strut. This method resulted in a significantly lower drag coefficient (.52).

Finally in an attempt to combine all the drag reduction schemes, we tested two imaged models with screen on the rear window area attached to the strut by means of a sting. This combination produced a drag coefficient of .52. This is still 16 per cent higher than the Brown and Seemann drag coefficient of .45, but for our first series of experiments in this area we considered our value acceptable.

After spending  $1\frac{1}{2}$  years to reproduce the correct drag on a sphere and an automobile model in the towing tank, reliable aerodynamic interference tests could be performed. Proper spacing and relative displacement of the models was accomplished by using a small carriage.

Four 7 foot pieces of .25 inch thick angle iron are welded together to form a 7 foot rectangular tube with inside dimensions  $5.5 \times 3.5$  inches. Inside the tube

a 12 inch aluminum trolley rolls on 12 roller skate wheels. The wheels are positioned 4 on the top, 4 on the bottom, and 4 on the sides, so that the motion is confined in a direction parallel to the tracks. From the bottom of the trolley two 9 inch surface piercing struts of symmetric airfoil design with chord lengths of  $2\frac{1}{2}$  inches and aspect ratios of 3.8 are used to hold the two truck models. The struts can be set at any angle so that with the small carriage set at an angle  $\alpha$  to the flow, a zero angle to the carriage direction can still be maintained. The two struts are bolted to a  $\frac{1}{4}$  inch thick steel plate with rounded corners, which in turn is bolted to the top of one of the trucks. The two truck models were positioned 4.5 inches apart which corresponds to the position where the wheels would have been touching. The whole small carriage assembly can be positioned to any angle from  $0^\circ$  to  $30^\circ$  with respect to the direction of motion of the main carriage. Once the carriage is positioned properly, it is bolted rigidly down to its supports on the towing carriage. An isometric drawing of this can be seen in Figure 15. The trolley and truck system moves manually by cranking a winch system. A small winch with a 3 inch drum is bolted to the top of the small carriage. The winch uses  $\frac{1}{8}$  inch nylon cord which goes through a pulley at one end of the carriage and then fastens to the trolley. The winch has four cams that trip a micro-switch at four equal time intervals in

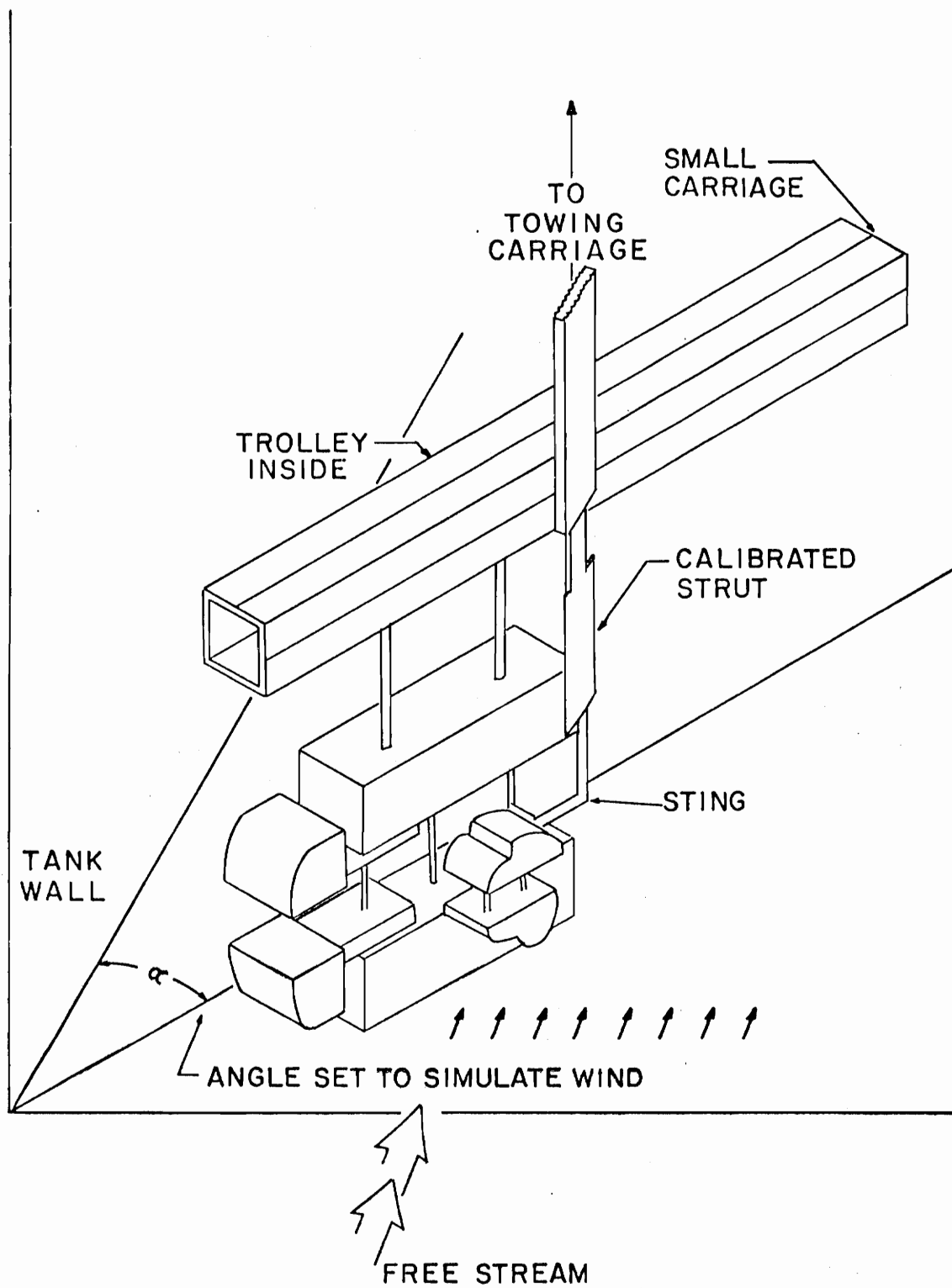


Figure 15. Isometric of car and truck arrangement

one revolution, and an event marker records these marks on our data paper. In this way the relative location of the two models is recorded next to the output of the strain gauges. Another micro-switch is set up to trip every time the truck's nose passes the nose of the automobile model. This is also recorded on our data paper, to locate the origin of relative displacement. The two other measured quantities were drag and side force of the car models, which were recorded on the same paper.

Three sets of data were taken with the car passing the truck. They correspond to three different horizontal spacings of  $1 \frac{1}{8}$ ,  $2 \frac{1}{4}$ , and  $3 \frac{3}{8}$  inches between the truck and Volkswagon models. These distances correspond to 8, 10, and 12 foot centerline spacing from the car to the truck in full scale. The relative position of the two models is given in terms of the coordinate system defined in Figure 16. The length of the car was used to nondimensionalize the longitudinal distance ( $X_s$ ) and the width of the car was used to nondimensionalize the relative lateral spacing ( $Y_s$ ). The relative spacings in these units then correspond to  $X$ ="car lengths," and  $Y$ ="car widths," so that lateral spacings of 8, 10, and 12 feet correspond to  $Y$  values of .3, .7, and 1.1 respectively. The towing carriage was run at 4 feet per second and the small carriage was set at an angle of  $24^\circ$  to the direction of motion. This angle was chosen to



simulate a 20 MPH cross wind on a 50 MPH truck. The car model was also set at  $24^\circ$  to the direction of motion by rotating its sting support by  $24^\circ$ , while the strut profile remained parallel to the flow. The car was on the downwind side of the truck, so that the Volkswagon model was shadowed by the truck.

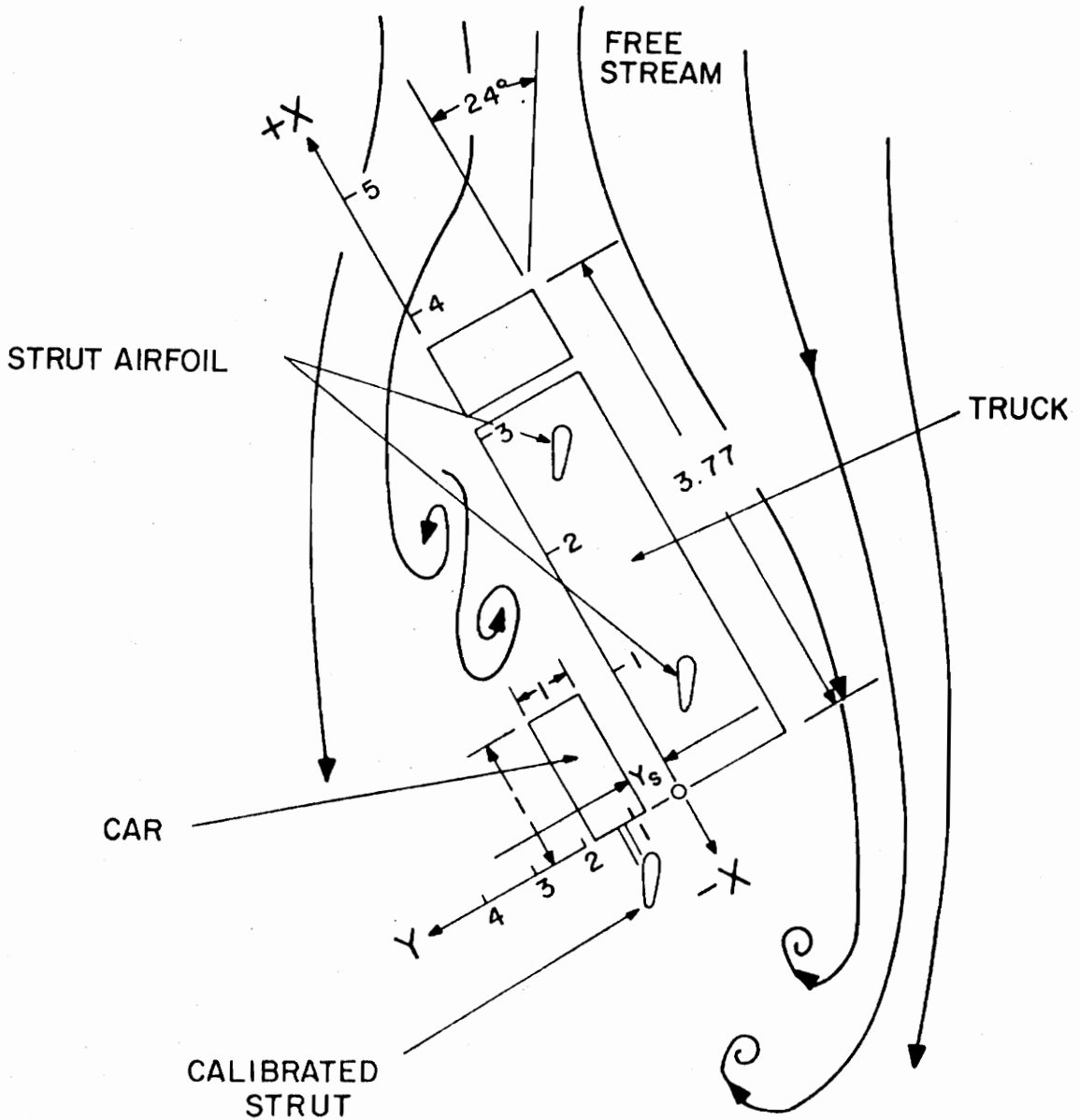
### c. Results and Discussion

To facilitate comparison with the work of Brown and Seemann, side force coefficients were calculated as follows

$$C_Y = \frac{F_Y}{1/2 \rho U_\infty^2 A}$$

where  $F_Y$  and  $C_Y$  are the side force and the corresponding coefficient respectively,  $1/2 \rho U_\infty^2$  is the dynamic pressure and  $A$  is the model frontal area. Distances were made dimensionless in the  $X$  and  $Y$  direction using the model length and width respectively. The coordinate system and a typical configuration of the experimental system is shown in Figure 16. Note that the distance  $X$  that measures the relative displacement of the two vehicles is zero when the nose of the car is next to the rear of the truck.

The present results as well as those of Brown and Seemann's are shown in Figure 17. This experiment simulates the passing process for car and truck speeds of 70 and 50 MPH respectively with a 20 MPH cross wind.



NOTE : ALL MEASUREMENTS ARE NONDIMENSIONAL

Figure 16. Car and truck spacings

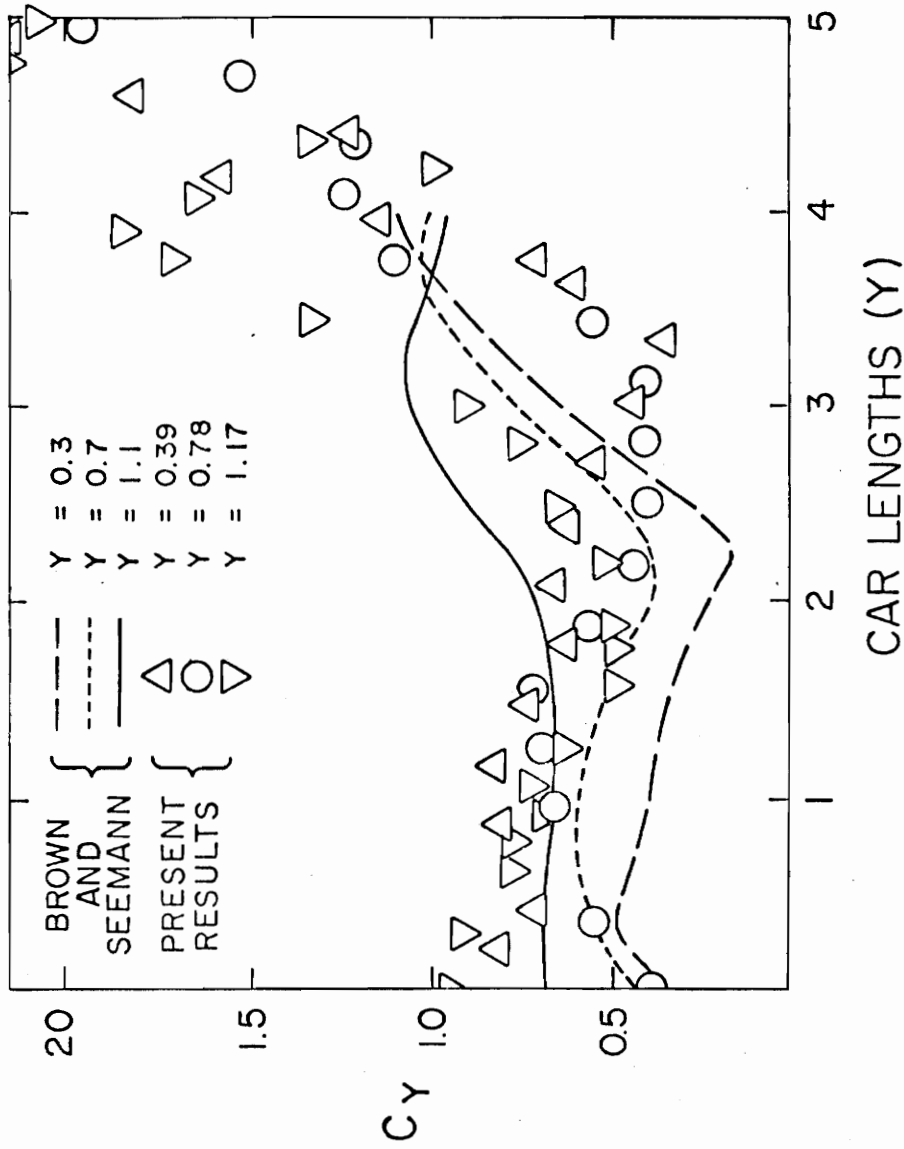


Figure 17. Interference side force coefficients simulating a passing process for three different spacings,  $Y$ , under the influence of a cross wind, with car, truck, and cross-wind speeds of 70, 50, and 20 MPH respectively

Brown and Seemann were able to take measurements for a large number of negative X's. Our experimental set up did not permit such measurements. However, we were able to take some measurements for  $X < 3.0$  which corresponds to a car moving in front of the truck, a regime that Brown and Seemann did not investigate. It appears that the present data are in reasonable agreement with the data of Brown and Seemann. Both investigations indicate an increase in the side force as the passenger car approaches the front of the truck. Brown and Seemann predict this trend a little earlier than the present method. This may be attributed to differences in the configuration of the cab. Both methods, and especially the present, indicate that the side force grows substantially as the passenger car is about to clear the truck. Two slight discrepancies are evident in the present data. The smallest separation ( $Y$ ) does not correspond to the lowest side force coefficient. This may be due to poor simulation of the ground effect by the method of images when the separation of the two vehicles is very small. Also, since the present data was taken with a slightly smaller truck model, the data around the truck's nose ( $Y=3.77$ ) should be shifted to the right approximately 0.13 car lengths, in order to be comparable to Brown and Seemann's data.

Drag was also rendered dimensionless by virtue of the dynamic pressure and the frontal area.

Drag coefficients are shown in Figure 18, again for three different separations of the two vehicles. Brown and Seemann did not measure drag coefficients and no other data is available for comparison. An interesting phenomenon emerges from the data of Figure 18. It appears that at  $X \approx 4.0$ , that is as the car is about to clear the truck, the drag coefficient increases to levels way above its undisturbed value. It is felt that this may be due to distortion of the wake shape and size due to the presence of the truck.

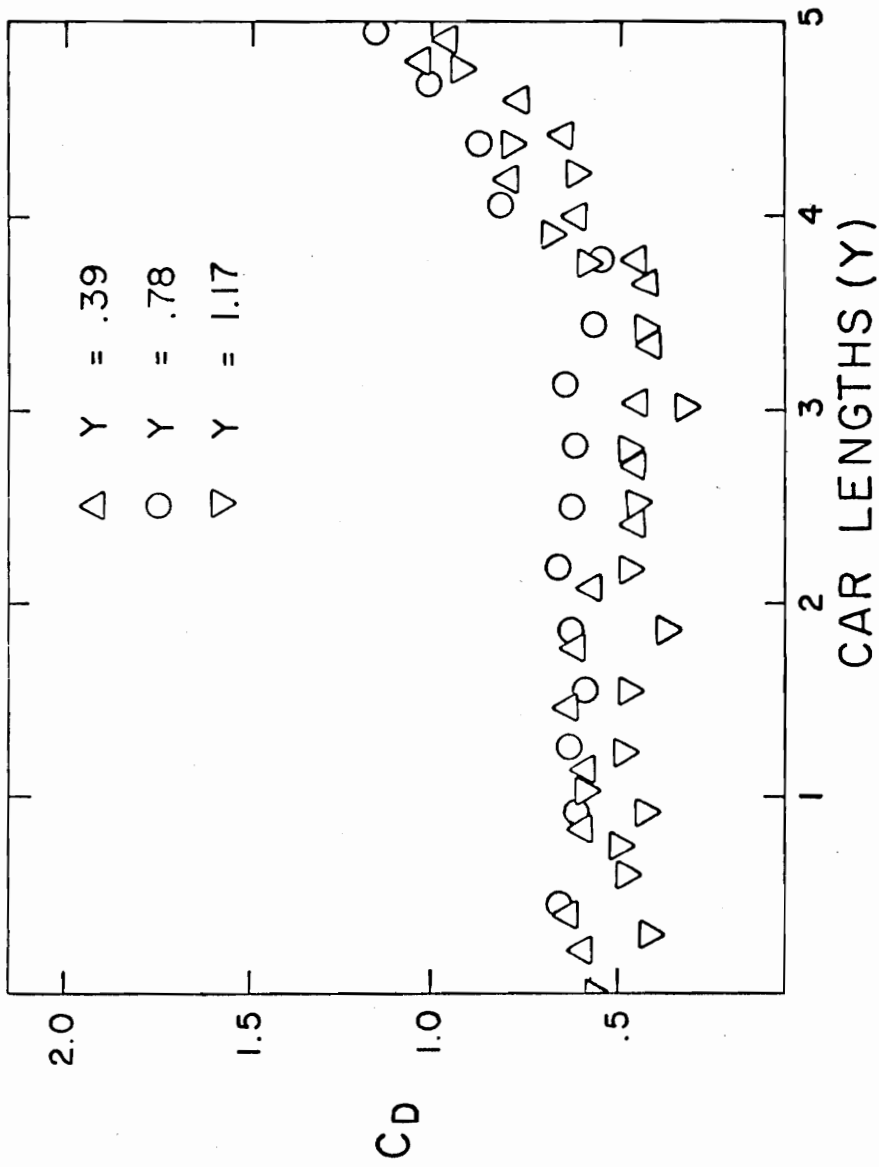


Figure 18. Interference drag coefficients for conditions of Figure 17

## CHAPTER IV

### CONCLUSIONS

The present experimental study has indicated that with proper balance systems and boundary-layer tripping devices it is possible to simulate high Reynolds number aerodynamic effects in a towing tank. It was demonstrated that the effects of walls and surface wave formation can be eliminated if the relevant distances are kept larger than at least half the width of the model.

Tests performed with highway vehicle models compare favorably with an earlier work in this area. This further proves that the experimental set up can be used to simulate successfully highway interferences between different vehicles. Tests were performed to simulate the passing process in the presence of a strong cross wind. It was discovered that the side-force coefficient increases substantially as the passenger car is about to clear the truck. More interesting is the behavior of the drag coefficient in the same neighborhood. It appears that the drag coefficient increases sharply to almost twice its undisturbed value. In other words, the passenger car experiences an extra component of drag as if the trailing truck is exerting an attractive force.

## REFERENCES

1. Lilienthal (1846 to 1896), *der vogelflug als grundlage der fliegekunst*, Belin 1889.
2. Mason, W.T., "Wind Tunnel Development of the Drag Foiler-a System for Reducing Tractor-Trailor Aerodynamic Drag," SAE Paper No. 750705.
3. Werle, H., "Hydrodynamic Flow Visualization," *Annual Review of Fluid Mechanics*, Vol. 5, pp.361-385, 1973.
4. Schraub, Kine, Henry, Runstabler, Little, "Use of Hydrogen Bubbles for Quantitative Determination of Time-Dependant Velocity Fields in Low Speed Water Flows," *TASME Report, Series D*, Vol. 87, June 1965.
5. Nychas, S.G., Hershey, H.C., Brodkey, R.S., "A Visual Study of Turbulent Shear Flow," *Journal of Fluid Mechanics*, Vol. 61, pp. 513-540, 1973.
6. Third International conference On Vehicle System Dynamics. Session 5, "Vehicular Aerodynamic Effects" chairman, J. Lukasiewicz, August 1974, Blacksburg, VA, sponsored by VPI & SU, ASME and Wayne State University.
7. Hoerner, S.F., Fluid Dynamic Drag, published by Author, 1965.
8. Reduction of Aerodynamic Drag of Trucks," NSF-RANN Conference, P. Lissaman, editor, Pasadena, CA, 1974.
9. Kamm, W.I.E., "Directional Stability of Motor Vehicles II, Stevens Institute of Technology, Technical Memorandum No. 103, September, 1953.
10. Toti, G., "Aerodynamic Effects on Vehicle Moving in Stationary Air and Their Influence on Stability and Steering Control," SAE Paper 948D, January, 1965.
11. Third International Conference on Vehicle System Dynamics, Session I, "Dynamics and Stability," chairman, P. Fancher, August, 1974, Blacksburg, VA, sponsored by VPI & SU, ASME and Wayne State University.



12. Dugoff, H., "On the Influence Of Aerodynamic Forces and Moments on the Lateral Stability on Articulated Highway Vehicles," proceedings of the First International Conference on Vehicle Mechanics.
13. Brown, G.J., and Seemann, G.R., "An Experimental Investigation of the Unsteady Aerodynamics of Passing Highway Vehicles" Report No. DOT-hs-800671, May, 1972.
14. Hawks, R.J., "The Effectiveness of Automotive Guidance in Reducing Automotive Cross-Wind Responce" from magazine Advances In Road Vehicle Aerodynamics 1973, edited by H.S. Stephens, published by BHRA Fluid Engineering.
15. Collier, M.L., "The Construction and Calibration of the VPI Towing Basin" taken from Virginia Polytechnic Institute Engineering Extension Series," Circular 7, June, 1966.
16. Streeter, V.L., and Wylie, E.B., Fluid Mechanics, published by McGraw-Hill Book Company, Copyright 1975.
17. "Modern Developments in Fluid Dynamics," edited by S. Goldstein, Vol. I, New York, Dover Publications Inc. 1965.
18. Telionis, D.P., "Calculations of Time-Dependant Boundary Layers," from Unsteady Aerodynamics, edited by Kinney, R.B., July, 1975.
19. Olson, R.M., Essentials Of Engineering Fluid Mechanics, Intext Education Publishers, New York and London, p. 204, 1973.
20. Behnert, R., Kleppe, K., H., and Roekmojoto, R., "Ground Effects for Jet Lift VTOL" NASA-TT-F-16359, 1972.
21. Fackrell, J.E., "The Simulation and Prediction of Ground Effects in Car Aerodynamics," Imperial College of Science and Technology, London UNIV., I.C. Aero Report 75-11, November, 1975.
22. "The Magnificent Turkey" from Petersons Complete Book Of Plymouth, Dodge, Chrysler, edited by S. Murray, 1973.

## VITA

The author was born in Cheverly, Maryland in March, 1952. He attended public schools in Rockville, Maryland, from 1956 until 1970. In September, 1970, he enrolled at Virginia Polytechnic Institute and State University where he participated in the Cooperative Education Program with the Naval Ship Research and Development Center in Carderock, Maryland. He received his B.S. Degree in Engineering Science and Mechanics in 1975. In September, 1975 he enrolled in the Engineering Science and Mechanics department of Virginia Polytechnic Institute and State University where he has been working towards his M.S. Degree.

A handwritten signature in cursive script, reading "Carl J. Fahrner", positioned above a horizontal line.

Carl J. Fahrner

AN EXPERIMENTAL INVESTIGATION  
OF FLUID DYNAMIC INTERFERENCE FORCES

BY

Carl J. Fahrner

(ABSTRACT)

Experimental investigations have been conducted in the VPI & SU towing basin to assess the feasibility of testing fully submerged configurations, simulating aerodynamic phenomena, and in particular, measuring aerodynamic interference force between blunt bodies. Special instrumented struts were constructed and calibrated for the measurement of drag and side forces. A series of tests were conducted with spherical models in order to verify the reliability of the method by comparison with earlier classical results. The effects of flat walls and surface wave formation were studied and it was discovered that their influence on aerodynamic forces is reduced to less than 10% if the body is removed from the wall or the surface by a distance larger than half its typical width. Experiments were also conducted with crude models that approximate the shapes of a passenger car and a truck. In particular, the passing process under the presence of a strong wind was simulated by towing the models at an angle of  $24^\circ$  with respect to motion of the carriage. The results appear to be essentially in agreement with the data received with much larger models tested in air, by other investigators.